International Journal of Industrial Electronics, Control and Optimization © 2022 IECO
Vol. 5, No. 2, pp. 153-165, April (2022)

# A New Enhanced Droop Controller for Seamless Load Sharing in AC Microgrids in Presence of Wind Turbine and Photovoltaic Sources

Sadegh Shajari[1], Reza Keypour[2, †]

[1,2] Department of Electrical and Computer Engineering, Semnan University, Semnan, Iran

ABSTRACT

*Load sharing, as an important challenge in microgrids (MGs), is realized commonly via a droop control method. Conventional droop control methods are not applicable in unpredictable renewable energy sources (RESs) like photovoltaic (PV) and wind turbines (WT) because their output power depends on the weather conditions and can be extracted only if these free sources are available. This paper considers two operating modes for these types of sources as Maximum Power Point Tracking (MPPT) and DC-link Voltage Control (DCLVC). These power sources usually operate in the MPPT mode unless the load of the MG drops to a lower level compared to the maximum power generation by RESs, in which case the sources switch to the DCLVC operating mode. This study proposed a method based on enhanced droop control, which helps RESs to choose their control mode locally without communication and share the demand of the AC MG with other dispatchable sources besides supplying its maximum power. The proposed method focused on supplying MG load from RESs as much as possible and simplicity in implementation. MG frequency helps the proposed controller to select its operation mode. Enhanced control for DC link voltage control is offered for inverter-based RESs. The validity of the proposed method is approved by simulations in the MATLAB/SIMULINK environment.*

**Article Info**

***Research Article***

***Keywords:***

Droop Method, Load Sharing, Microgrid (MG), Photovoltaic (PV), Wind Turbine (WT)

***Article History:***

**Received** 2021-09-18

**Accepted** 2022-04-12

## I. INTRODUCTION

Since greenhouse gas reduction has become an important environmental issue, renewable energy resources (RESs), such as wind and solar energy, have gained huge attention, especially in MGs [1], [2]. Integration of RESs and MGs requires power electronic interfaces [3], [4]. Hence, MGs comprise of RESs, energy storage systems, and power electronic interfaces. To share MG's load among parallel power electronic interfaces, suitable control methods should be applied to avoid circulating currents, especially in presence of RESs [5] – [7].

In the future, many countries around the world are likely to experience high penetration levels of WT and PV as RESs, to not only reduce greenhouse gas emissions but also utilize an interesting economic alternative in areas with abundant wind or solar radiation. The integration of high penetration levels of WT and PV into MGs may require new approaches and solutions [8], [9]. Due to the intermittency effect and renewable characteristics, WT and PV units can operate in either MPPT or DCLVC mode, while other dispatchable sources have the linear droop characteristic.

Basically, the first solution is to employ a central controller, that is why the authors in [10] propose a central controller to control the PV output power in an MG. Supplying unbalanced load via the combination of PV and battery energy storage system in [11] and [12] is another example indicating an effort to control RESs via a central controller. High bandwidth is critical for central controllers in an MG. The costs of high bandwidth infrastructure besides noise and network security make the central controller an undesirable option and weakness of the mentioned papers. That is the reason researchers tend to use local controllers.

[†]**Corresponding Author**: rkeypour@semnan.ac.ir
Tel: +98-2331532724, Fax: +98-31532699, Semnan University
Faculty of Electrical and Computer Engineering, Semnan University, Semnan, Iran

Copyright © 2022 Keypour et al. Published by University of Sistan and Baluchestan. This work is licensed under a Creative Commons Attribution-Noncommercial 4.0 International license. (https://creativecommons.org/licenses/by-nc/4.0/). Non-commercial uses of the work are permitted, provided the original work is properly cited

Although the increase in the RESs penetration in MGs is intended and desirable, DC MGs are preferred because of their less complexity. That is why authors in [13] and [14] apply a voltage droop control to a DC MG. In [15], an integrated PV and battery energy storage are controlled based on the voltage of a DC MG. Also, the authors in [16] propose the supervisory control for a combination of PV and WT along with a battery energy storage device for a DC MG. Although the mentioned literature proposes a control method for RESs in DC MGs, dispatchable sources besides RESs do not share the load with each other. Hence not involving load sharing in the study is a disadvantage of their methods. In [17], a decentralized control method based on the V-I droop concept is proposed for multiple PV sources, where the objective is to regulate the DC bus in a DC MG. Despite the fact that power sharing among PV sources has been carried out in some studies, PV sources cannot operate in the MPPT mode, unless a DC MG is in connected grid connected mode and that is the weakness of the study.

Some authors tried to control RESs in AC MGs, where the droop control method was used to control PV sources to improve the MG voltage at the fundamental frequency [18]. In another study, a control method is proposed for a PV source so that it could operate in grid-connected or standalone mode, but load sharing in presence of RESs is not discussed because multi-source MGs were discarded [19]. Load-sharing in the studies is still not addressed, which is the weakness of the above studies. Most papers addressing the load sharing in AC MGs are focused on dispatchable sources while neglecting RESs [20] – [22]. Due to intermittent characteristics of RESs, load sharing of the proposed paper does not have the capability of controlling RESs. There are few studies that discuss the effects of RESs on load sharing. In [23], autonomous control strategies are proposed for PV and battery units operating in a droop-controlled islanded MG based on PV. Authors in [24] present a local controller for a single PV source to share its power and a dispatchable source power, in which the intermittent effect of RESs is considered in the AC MG. Nonetheless, it can be used only for MGs with a single PV source. References [25] and [26] introduce a decentralized controller for load sharing of a hybrid PV/Battery source based on switching between different operating modes. Yet, due to switching between numerous modes, an unpleasant transient is inevitable and it is the foible of the method. Considering the mentioned studies, further investigation is required to analyze the load sharing in intermittent RESs, especially in WTs of AC MGs.

The present study proposed a decentralized controller to select the operating mode of the RESs based on local measurements and a droop method. MG frequency is used as a switching criterion between operation modes. The proposed controller helps RESs to extract the maximum power and supply the MGs in the MPPT mode. During low load conditions, the DCLVC mode is activated in the RESs to control DC link voltage in RESs and, while other dispatchable sources provide their minimum power, RESs share MG's load among each other, and power curtailment might occur if it is necessary. A comprehensive controller is proposed for DC link voltage control in PV and WT sources. It has the responsibility for determining the amount of power curtailment according to the voltage level of the DC link voltage. The power curtailment method varies according to the type of source.

The organization of the paper is as follows. The primary control and proposed decentralized controller are explained in sections II and III, respectively. Simulation results are provided in section IV, and the last section presents the conclusions.

## II. PRIMARY CONTROL

Various types of power sources are connected to MGs. They may operate in stand-alone or grid-connected mode. Fig. 1 shows that power sources, such as PVs, WTs, or battery energy storage devices, are connected to MG by DC/AC power electronics interfaces in a sample structure of the MG. Voltage Source Inverter (VSI) and Current Source Inverter (CSI) are usually used as DC/AC interfaces between the source and the MG. Thanks to the ride-through and power quality advantages, VSIs have gained more attention in MGs applications [27], [28].

Current control loops, voltage control loop, virtual impedance loop, and droop control of VSI primary control are depicted in Fig. 2. The voltage control loop is responsible for voltage stability, especially in RESs-based MGs. Current control is in charge of continuous current injection with eliminated harmonics, especially in low-order harmonics. Current tracking must have a high bandwidth because it should provide a faster response than the voltage control; otherwise, any voltage disturbance can lead to an increase in the current THD and result in instability [29].

The proportional integral (PI) controller is the most widely used controller in inverter controls, but the proportional resonant (PR) controller is becoming more popular because of its faster dynamic response, higher gain at the fundamental frequency, and less harmonic components, especially in low-order harmonics.

The frequency and amplitude of the reference voltage are calculated based on frequency-active power and amplitude–reactive power relationships in the droop control method. Virtual impedance is added to make up the line impedance effect and reduce the dependency of active power and reactive power to voltage, and frequency, respectively [30]. Secondary control is responsible for the compensation of primary control deviation [31].

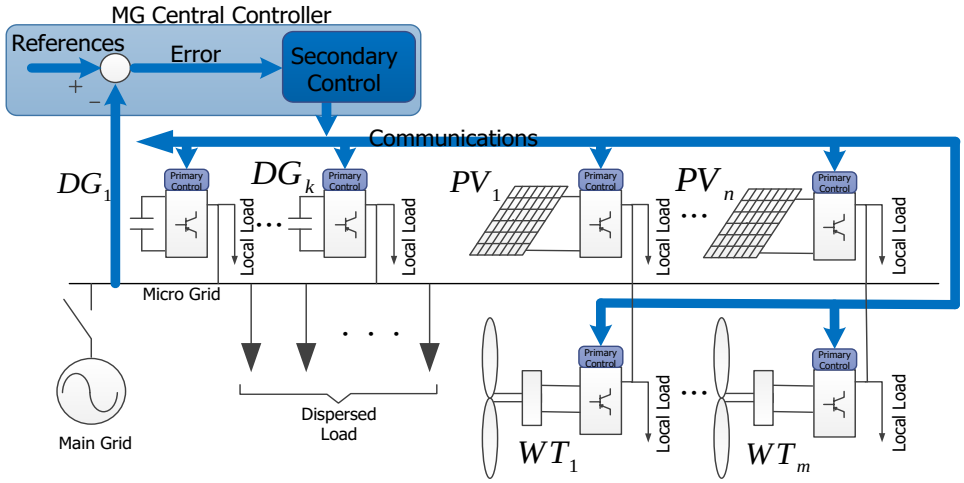



**Fig. 1**. Structure of an MG

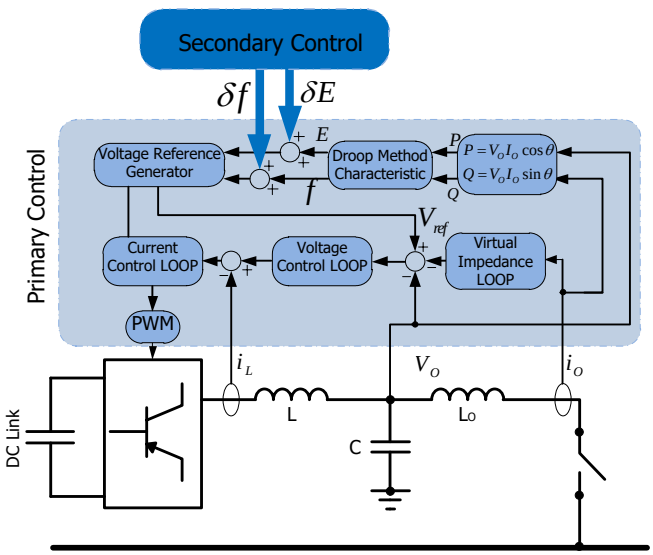



**Fig. 2**. Control of a DG source in an MG

## III. PROPOSED METHOD

The sample AC MG depicted in Fig. 3 is used for the study. As Fig. 3 shows, the considered AC MG consists of 'm' number of WT sources, 'k' number of battery energy storage sources and 'n' number of PV sources. PV sources are connected to the AC MG through a DC/DC converter and a DC/AC inverter. The DC/DC converter is responsible for the maximum power point tracking. The DC/AC inverter is used in the WT. The MG load is converted to an integrated single load.

Load sharing in the sample MG is usually performed by the droop control method, which is described by the following equations:

$$\begin{aligned} \omega_{PVi} &= \omega^*_{PVi} - D_{PVi}(s)P_{PVi} \qquad 0 \le i \le n \\ \omega_{WTj} &= \omega^*_{WTj} - D_{WTj}(s)P_{WTj} \qquad 0 \le j \le m \\ \omega_h &= \omega^*_h - D_h(s)P_h \qquad 0 \le h \le k \end{aligned} \tag{1}$$

where, $\omega^*_{PVi}$, $\omega^*_{WTj}$, and $\omega^*_h$ are angular frequency references and $D_{PVi}$, $D_{WTj}$ and $D_h$ represent frequency droop coefficients.

$$\begin{aligned} E_{PVi} &= E^*_{PVi} - D_{Q-PVi}(s)Q_{PVi} \qquad 0 \le i \le n \\ E_{WTj} &= E^*_{WTj} - D_{Q-WTj}(s)Q_{WTj} \qquad 0 \le j \le m \\ E_h &= E^*_h - D_{Q-h}(s)Q_h \qquad 0 \le h \le k \end{aligned} \tag{2}$$

where, $E^*_{PVi}$, $E^*_{WTj}$ and $E^*_h$ show voltage references, and $D_{Q-PVi)}$, $D_{Q-WTj}$ and $D_{Q-h}$ denote voltage droop coefficients.

The conventional droop method should be developed to be applicable to renewable intermittent sources like PVs or WTs. Hence, a new method is proposed here, with two operating modes as illustrated in Fig. 4 (a). Two control modes, one corresponding to the droop section of the curve and the other one corresponding to the vertical section of the curve in Fig 4. While the system frequency remains between $f_{DS}$ and $f_{min}$, renewable intermittent sources which may be PV sources or WTs track the maximum power and deliver it to the MG and operate in the MPPT mode (vertical section). As shown in Fig. 4 (a), the maximum power can be changed according to the weather variations and the remaining load shares among dispatchable sources. When the frequency of the MG increases to a higher level compared to $f_{DS}$, dispatchable sources deliver their minimum power due to the load decrease, and intermittent sources share the load among each other based on a droop characteristic, which depends on the maximum extractable power of each available source according to the droop section of Fig. 4.

Fig. 5 depicts different operating modes of the proposed method in the sample AC MG with two PV sources, one WT source, and one dispatchable source. At State 1, each source delivers its maximum available power to the MG. Decreasing the load in this mode leads to a power decrease in the dispatchable source while renewable intermittent sources still operate at the maximum power point (MPP). When frequency reaches $f_{DS}$ and the MG operates at State 2, the dispatchable source operates at its minimum power mode and RESs are in charge of supplying the load. Increasing the frequency to State 3 leads to power curtailment in RESs and the DCLVC is activated in RESs to properly decrease their output power. At State 3, RESs share the load of the MG among each other using a new droop characteristic based on the maximum available power of each source.

Since the proposed characteristic includes both MPPT and DCLVC modes, each part should be covered in a separate section.

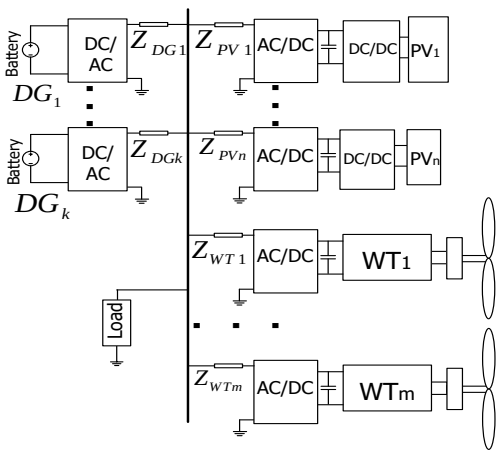



**Fig. 3.** Configuration of the system under study

### A. *Maximum Power Point Tracking Control Mode*

This mode is an important mode [32], [33] and RESs track their maximum power points and frequency of the MG is lower than $f_{DS}$. Thus, the active power equation should be modified as follows:

$$\begin{aligned}\omega_{PVi} &= \omega^*_{PVi-New} - D_{PVi}(s)P_{PVi}\\ \omega_{WTj} &= \omega^*_{WTj-New} - D_{WTj}(s)P_{WTj}\\ \omega_h &= \omega^*_h - D_h(s)P_h\end{aligned} \tag{3}$$

Where, $\omega^*_{PVi-New}$ and $\omega^*_{WTj-New}$ are new angular frequency references obtained from Equ. (4):

$$\begin{aligned}\omega^*_{PVi-New} &= \omega^*_{PVi} + \frac{D_{PVi}(s)}{S}\left(P_{Max-PVi} - P_{PVi}\right)\\ \omega^*_{WTj-New} &= \omega^*_{WTj} + \frac{D_{WTj}(s)}{S}\left(P_{Max-WTj} - P_{WTj}\right)\end{aligned} \tag{4}$$

Equ. (4) helps RESs to deliver their maximum power to the MG with updating character.

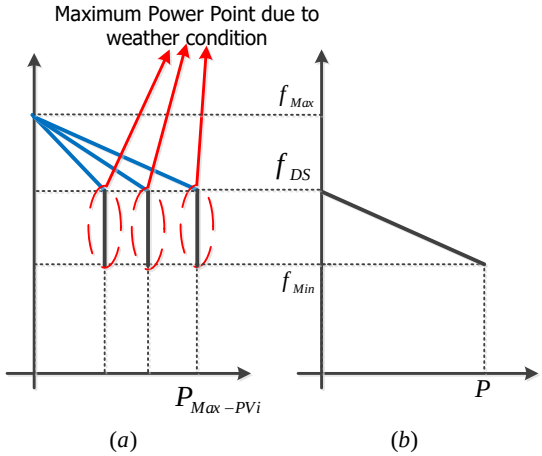



**Fig. 4.** The proposed characteristic for an intermittent renewable source (a) beside a conventional droop (b)

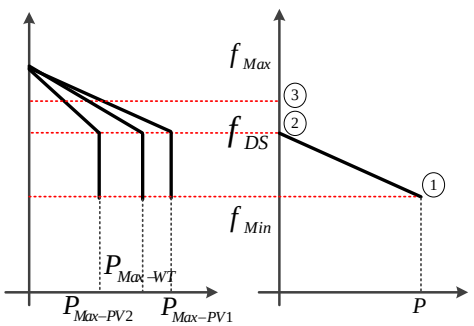



**Fig. 5.** Operation of the proposed method in different states

Active power and phase angle relationships are similar in all sources. The relationship between the active power of inverter 'i' belonging to the PV source and its phase angle is given by Eq. (5) [33]:

$$\begin{aligned}\left(\delta_{PVi} - \delta_{com}\right) &= \int\left(\omega_{PVi} - \omega_{com}\right)dt\\ P_{PVi} &= \frac{E_{PVi}V_{com}\sin\left(\delta_{PVi} - \delta_{com}\right)}{X_{PVi}}\end{aligned} \tag{5}$$

Where, $E_{PVi}$ is the output voltage magnitude of the *i*th inverter $V_{com}$ is the common bus voltage magnitude, and assuming inductive impedance of line, $X_{PVi}$ is the connection inductance.

Small signal analysis is necessary for the adjustment of control parameters. Linearization of Equs. (3) - (5) at a single operating point leads to:

$$\begin{cases}\Delta\omega_h = \Delta\omega^*_h - D_{h(S)}\Delta P_h\\ \Delta\omega_{PVi} = \Delta\omega^*_{PVi-New} + \dfrac{D_{PVi(S)}}{S}\left(\Delta P_{Max-PVi} - \Delta P_{PVi}\right)\\ -D_{PVi(S)}\left(\Delta P_{PVi}\right)\\ \Delta\omega_{WTj} = \Delta\omega^*_{WTj-New} + \dfrac{D_{WTj(S)}}{S}\left(\Delta P_{Max-WTj} - \Delta P_{WTj}\right)\\ -D_{WTj(S)}\left(\Delta P_{WTj}\right)\end{cases} \tag{6}$$

$$\begin{cases} (\Delta\delta_h - \Delta\delta_{com}) = \int (\Delta\omega_h - \Delta\omega_{com})dt \\ (\Delta\delta_{PVi} - \Delta\delta_{com}) = \int (\Delta\omega_{PVi} - \Delta\omega_{com})dt \\ (\Delta\delta_{WTj} - \Delta\delta_{com}) = \int (\Delta\omega_{WTj} - \Delta\omega_{com})dt \end{cases} \quad (7)$$

$$\begin{cases} \Delta P_h = G_h (\Delta\delta_h - \Delta\delta_{com}) \\ \Delta P_{PVi} = G_{PVi} (\Delta\delta_{PVi} - \Delta\delta_{com}) \\ \Delta P_{WTj} = G_{WTj} (\Delta\delta_{WTj} - \Delta\delta_{com}) \end{cases} \quad (8)$$

$$G_h = \frac{E_h^i V_{com}^i \cos(\delta_h^i - \delta_{com}^i)}{X_h}$$

$$G_{PVi} = \frac{E_{PVi}^i V_{com}^i \cos(\delta_{PVi}^i - \delta_{com}^i)}{X_{PVi}} \quad (9)$$

$$G_{WTj} = \frac{E_{WTj}^i V_{com}^i \cos(\delta_{WTj}^i - \delta_{com}^i)}{X_{WTj}}$$

The control block diagram for RESs and the dispatchable source is illustrated in Fig. 6. As the small signal model of all RESs is similar, small signal model of one PV source is depicted as an example. A low-pass filter with a cut-off frequency of 0.2 Hz is considered in the control block of all sources. The filter is represented by $G_{LPF(S)}$, and a PI controller is used for droop control as represented in Equ. (11) [30]:

$$G_{LPF(S)} = \frac{1}{1+\tau_p S} \quad (10)$$

$$D_h, D_{PVi}, D_{WTj} = \frac{K_{pP}S + K_{iP}}{S} \quad (11)$$

According to Ref. [27], the characteristic equation can be extracted from Fig. 6. In Fig. 7 root locus of the model is depicted. As all the three poles stay on the left side, the stability of the proposed method is confirmed. The conventional voltage-reactive power droop is applied to the reactive power control [30].

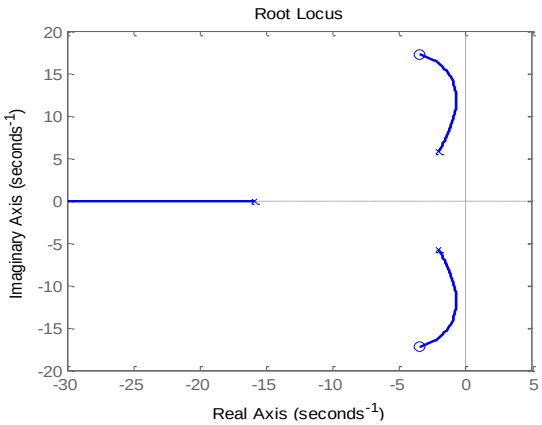



**Fig. 7.** Root locus for small signal analysis in MPPT mo

## B. DC-link Voltage Control Mode

When the load of the MG decreases to a lower level compared to the total maximum power of the RESs and dispatchable sources operate in a minimum power state, power curtailment is inevitable in RESs. The DC-link voltage will increase beyond its permissible maximum voltage due to the difference between the injected power to the DC-link and extracted power from it. Hence, RESs should switch from the MPPT mode to the DCLVC mode to control the DC-link voltage by controlling the power injected into the DC-link.

As there are two types of RESs in this study, two types of a controller are proposed for the DC-link voltage control of PV and WT units, as shown in Figs. 8 and 9. These two controllers operate similarly but with minor differences. In both of them, the difference between the DC-link voltage and the permissible maximum voltage passes through the saturation block. If the difference value is positive, the saturation block saturates the output at zero, and the voltage controller for DC/DC converter in PV source or pitch

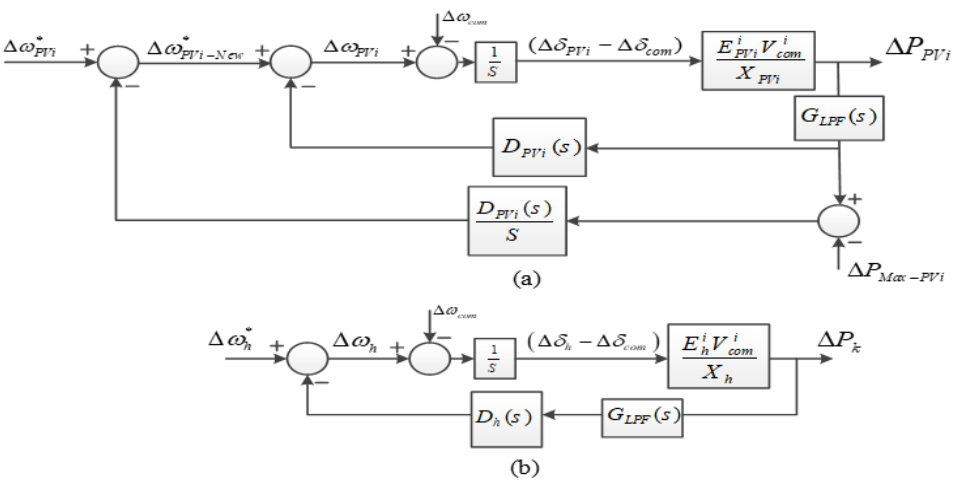



**Fig. 6.** Small signal model of the active power control in the MPPT mode (a) active power control controller in of RESs, and (b) active power control of the dispatchable source

WT source works to seek maximum power. When the difference value is negative, the output of the compensators, which are PI controllers, will be added to the output of the MPPT controller or the pitch angle controller. Therefore, the output of the DC/DC converter or the pitch angle controller does not track the maximum power and is changed to fix the DC-link voltage at the permissible maximum voltage.

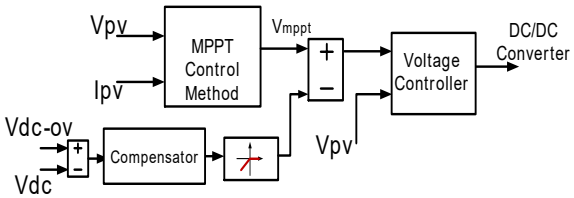



**Fig. 8.** Block diagram of the DC/DC converter control

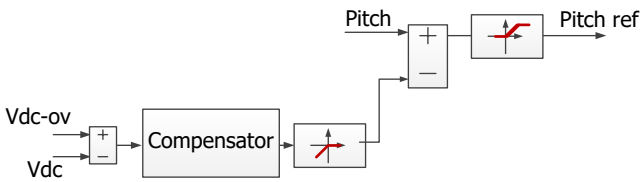



**Fig. 9.** Block diagram of the AC/DC rectifier control of the WT

As power curtailment is happening in this state and power is shared among RESs based on the new droop control, the droop equation for RESs changes as follows:

$$\omega_{PVi} = \omega^{*}_{PVi} - D_{PVi-New} P_{PVi}$$
$$\omega_{WTj} = \omega^{*}_{WTj} - D_{WTj-New} P_{WTj} \quad (13)$$

New droop coefficients can be calculated by Equ. (14).

$$D_{PVi-New} = \frac{f_{\max} - f_{DS}}{P_{Max-PVi}}$$
$$D_{WTj-New} = \frac{f_{\max} - f_{DS}}{P_{Max-WTj}} \quad (14)$$

Similar to the previous section, small signal can be obtained. This is shown in Fig. 10 for the PV as an example.

### *C. Mode Detection*

Fig. 11 shows how the proposed controller works locally and chooses its control mode for the PV source. The control method for WT is the same. According to Fig. 4, $f_{DS}$ is a border between two operating modes. Equation (15) shows the calculation of $f_{DS}$ for an MG. Thus, when the system frequency is higher than $f_{DS}$, the proposed controller locally chooses the DCLVC mode and if it is lower than $f_{DS}$, the MPPT mode is selected. Consequently, the system frequency passes through two saturation blocks with inverse operation modes and the outputs are multiplied by the reference voltage values. Finally, the sum of multipliers outputs produces reference voltage. Therefore, when the frequency of the MG is lower than $f_{DS}$ , the reference voltage is the product of the MPPT mode, else it will be the product of the DCLVC mode.

$$f_{DS} = \frac{Dispatchable\ \ Power(f_{Max} - f_{Min})}{Dispatchable\ \ Power + Renewable\ \ Power} + f_{Min} \quad (15)$$

## IV. Simulation Results

Simulation of the proposed method is performed in the MATLAB/Simulink environment to show its validity. Fig. 12 illustrates the sample AC MG, in which two PV sources, one WT source, and one dispatchable source are used for simulation purposes. The WT consists of an induction generator, a gearbox, and a wind turbine all interconnected. As Matlab Simulink environment is used for simulation, the default model of wind turbine beside some modifications from [8] and [9] are used for modeling the wind turbine. The maximum power of PV sources below 1000 W/m$^2$ irradiation is shown in Table I. Method of [34] and [35] is used for PV power extraction. The Maximum power of the WT source below 10 m/s wind speed and zero pitch angle is provided in Table I. An LC filter at the output of the inverter is connected to all sources. Control parameters for all sources are provided in Table I. Common parameters for all sources have the same values. The load of the MG load is varied in a way that all operating modes can be achieved. The maximum and minimum frequencies of the MG are 50.1 Hz and 49.9 Hz, respectively. Hence, $f_{DS}$ is roughly 49.96 Hz in the MG with the power in Table I.

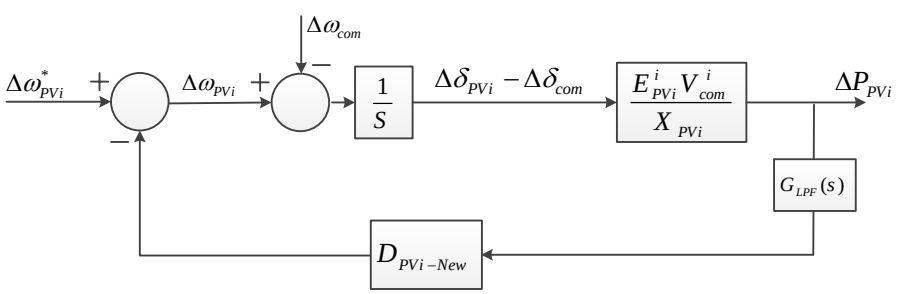



**Fig. 10.** Small signal model for active power control in the DC-link voltage control mode for the RESs.

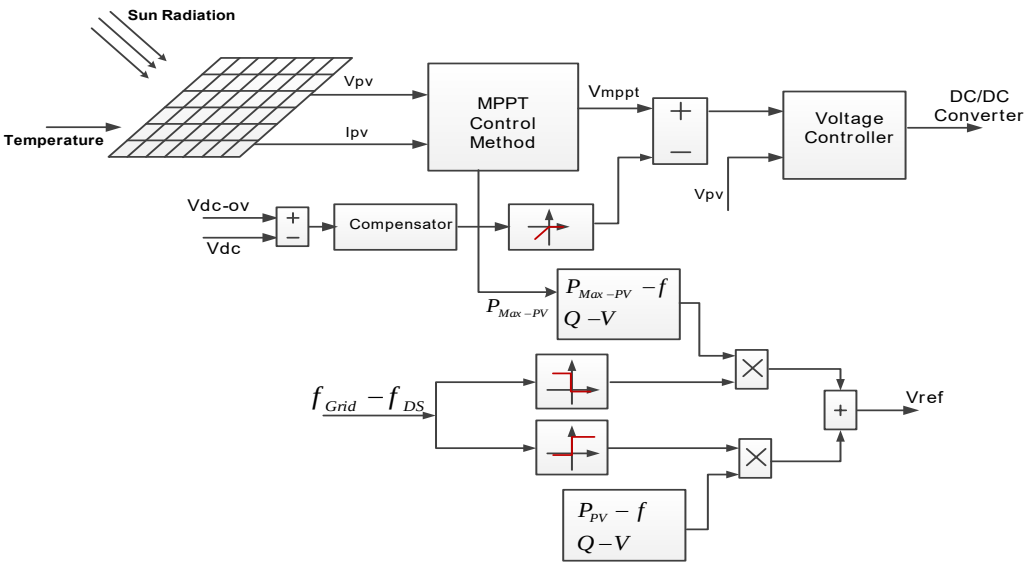



**Fig. 11.** The proposed control method

Simulations under different situations are performed. Changes in the load and weather conditions are investigated in the first and second simulations, respectively. The first simulation starts under 1000 $\frac{W}{m^2}$ irradiance for PV sources, 10 $\frac{m}{s}$ wind speed for the WT source, and the MG load equal to 3400 W. Then the MG load decreases two times; in the first case, the load reaches 3100 W at t = 5 s (section 2 in Fig. 13) and in the second case, it decreases to 2200 W at t = 10 s (section 3 in Fig. 13). In the next step, the MG load increases and reaches 2600 W at t = 30 s (section 4 in Fig. 13).

As expected, when the MG load is 3400 W, the frequency drops below $f_{DS}$ and all RESs deliver maximum reachable power to the MG and the remaining load is supplied by the dispatchable source, which is shown in section 1 in Fig. 13 and Fig. 14. At t = 5 s, the MG load decreases and the frequency increases to a higher level to become almost equal to $f_{DS}$ . Therefore, the dispatchable source power decreases to its minimum power state, while RESs still deliver maximum power to the MG. More decrease in the MG load leads to more increase in the MG frequency. Thus it is expected that the frequency increases to a higher level compared to $f_{DS}$ and RESs change the control mode from the MPPT to the DCLVC mode, and power curtailment happens. Section 3 of Fig 13 illustrates the proposed controller reaches the predetermined goals and load sharing during DCLVC mode is properly performed. Fig 15 shows the DC-link voltage for RESs. Different maximum permissible voltages are considered for each source to check each source separately. According to Fig. 13 and Fig. 15, RESs share the load between each other in a very proper manner and the DC-link voltage is kept constant at permissible maximum voltage. The DC-link voltage variation of PV1 and PV2 is similar and the controller response is very fast. However, in the case of the WT, it is much slower because of mechanical mechanism dynamics. The controller changes the pitch angle and due to a higher time constant and a slower response of the pitch control system, the variations in the DC-link voltage in the WT are much slower compared to those of PV sources.

**Table I**
SIMULATION PARAMETERS

| Type | Symbol | Quantity | Value |
|---|---|---|---|
| Electrical Parameter | $V_{MG}$ | MG voltage | 311 V |
| | f | MG frequency | 50 Hz |
| | $V_{DC}$ | DC voltage | 650 V |
| | $P_{Max-PV1}$ | PV1 Maximum Power | 1.4 kW |
| | $P_{Max-PV2}$ | PV2 Maximum Power | 0.7 kW |
| | $P_{Max-WT}$ | WT Maximum Power | 1 kW |
| | $P_{Max-Dispatch}$ | Dispatchable Source Maximum Power | 1.35 kW |
| | C | Filter Capacitance | 25 $\mu f$ |
| | L | Filter Inductance | 1.8 mH |
| | $L_O$ | Output Impedance | 1.8 mH |
| Inner Loops | $K_{pI}$ | Current proportional term | 0.35 |
| | $K_{iI}$ | Current Integral term | 200 |
| | $K_{pV}$ | Voltage proportional term | 0.35 |
| | $K_{iV}$ | Voltage integral term | 400 |
| Droop Control | $K_{pP}$ | Active power droop coefficient | 0.00001 ($^{Rad}/_{W.}$ |
| | $K_{iP}$ | Active power droop Integral term | 0.0008 ($^{Rad}/_{W.s}$ |
| | $K_{pQ}$ | Reactive power droop coefficient | 0.16($^{V}/_{Var}$) |
| | $R_V$ | Virtual Resistance | 1 Ω |
| | $L_V$ | Virtual Inductance | 4 mH |

At t=30 s, the MG load increases and makes the MG frequency decrease but it is still higher than $f_{DS}$, therefore DCLVC is ON and power curtailment happens again. Due to a sudden increase in the output power, the DC-link voltage

experiences a sudden decrease but power from RESs compensate for the changes, and the DC-link voltage returns to its previous state immediately.

As the controller has online maximum power tracking, it should have the ability to respond to any changes in weather conditions. So, in the second simulation case, irradiance and wind speed changes are considered to examine the response of the proposed controller.

In the second simulation, the MG load is kept constant and irradiance for the PV1 is decreased from 1000 $\frac{W}{m^2}$ to 500 $\frac{W}{m^2}$ at t = 10 s, then it is increased to 1000 $\frac{W}{m^2}$ at t = 20 s. Wind speed change occurs at t = 30 s and t = 40 s for the WT. At t = 30 s, wind speed is decreased from 10 $\frac{m}{s}$ to 8 $\frac{m}{s}$ and at t = 40 s it becomes 10 $\frac{m}{s}$. Fig. 16 shows active power variation of all sources while the MG load is 3400 W and kept constant while weather conditions are changed for some of the RESs. As depicted in section 2 of Fig. 16, when irradiance changes from 1000 $\frac{W}{m^2}$ to 500 $\frac{W}{m^2}$ for PV1, as expected the MPPT controller finds a new maximum power, and the output power of PV1 decreases to 50 percent of its nominal power. While other RESs deliver their maximum power, the dispatchable source has the free capacity to compensate for differences between the MG load and the generation. So, the output power of the dispatchable source increases to make up the difference. When irradiance increases to 1000 $\frac{W}{m^2}$ at t = 20 s in section 3 of Fig. 16, the MPPT of PV1 changes its operating point to a previous state, and as it is predictable the output power of PV1 increases to its nominal power, hence the dispatchable source power drops to its previous state. The response of the WT to a decrease in the wind speed is shown in section 4 of Fig. 16, in which the wind speed decreases to 8 $\frac{m}{s}$ at t = 30 s. It can be guessed that the dispatchable source takes the responsibility for the generation and load difference by increasing its output power. As depicted in section 4 of Fig.16, the dispatchable source makes up the difference. Section 5 shows the return to the previous state when the wind speed increases and the dispatchable source power decreases to its initial state. Figs. 17 and 18 show the frequency of the MG and variations in DC-link voltages of all RESs. Although irradiance or wind speed has been changed during the second simulation, the power injected into the DC-link and power extracted from DC- link was almost equal during weather changes for all RESs. Hence, the DC-link voltage did not experience much variation due to weather changes. MG voltage variation due to weather change is illustrated in Fig. 19. As shown in Fig. 19, changes in solar radiation or wind speed, which are accompanied by changes in the output power of REVs, cause changes in the MG voltage. Of course, the performance of the reactive power controller, which is responsible for the MG voltage control, is quite satisfactory and has a good speed to power changes.

load sharing with the conventional droop method is performed in Fig. 20 to compare with the proposed controller operation. Weather variation is the same as Fig. 16. As depicted in Fig 20, load sharing performed very well but the dispatchable source share is increased compared to Fig. 16. Hence extracting power from RESs is decreased and RESs do not work at MPPT under any circumstances. As previously mentioned, the conventional droop method is not suitable for use with RESs.

In order to check the effectiveness of the proposed method, simultaneous change in load variation and weather change is applied. At t=15 s load decreased from 3400W to 3000W and sun radiation for PV1 decreased to 500 $\frac{W}{m^2}$ from 1000 $\frac{W}{m^2}$. Again at t=30 s load decreased to 2300W and wind speed from 10 $\frac{m}{s}$ reduced to 8$\frac{m}{s}$ . Fig. 21 shows that even in the simultaneous change of load and weather, the proposed controller properly shares the MG load among sources and insists on supplying load from RESs by helping them to work in MPPT mode.

## V. CONCLUSION

This study shows that the proposed controller is applicable in renewable inverter-based sources with the DC-link voltage. It helps RESs to select their control mode locally using the MG frequency. Thus, the communication link can be omitted or lower bandwidth communication with much less cost can be used instead. Any decrease in dependency on communication will increase the reliability of the system and reduce the noise influence on the operation of the controller.

Due to insist of the proposed method on consuming maximum reachable power of renewable source unless MG is in low load condition and cannot absorb the power, greenhouse gas emission reduces and penetration of renewable sources such as PV and WT in AC MG grows.

Simulation results show that the operating mode is identified very well with the help of local measurements and the response of RESs to the MG load changes is very fast. Usage of the proposed method with PV and WT confirms that the proposed method is capable of matching with different types of RESs and the maximum power point tracking method.

It is recommended to consider battery state of charge or DC link voltage level in power sharing during DCLVC mode for future work. RESs with a low level of DC link voltage can absorb power and act as a load during low load conditions and power curtailment can be reduced. It helps to use more renewable power. Load management can be investigated in future work when MG's available power is less than MG demand.

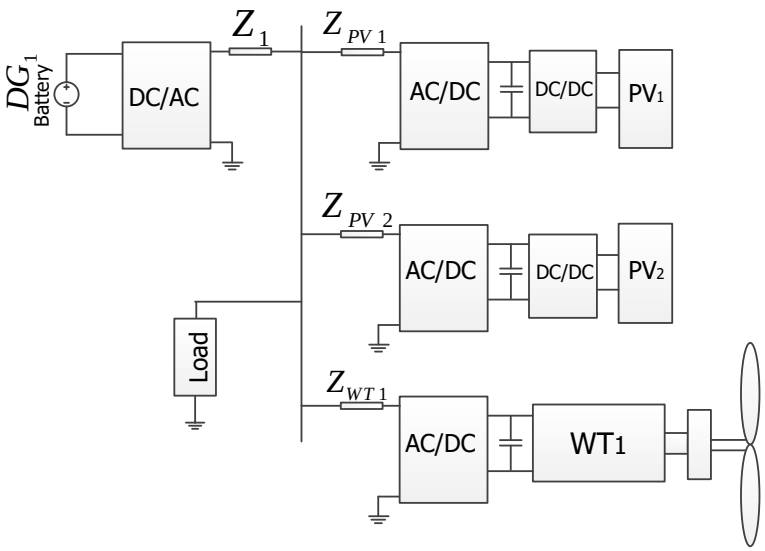



**Fig. 12.** A sample AC MG with three RESs and one dispatchable source used in simulations

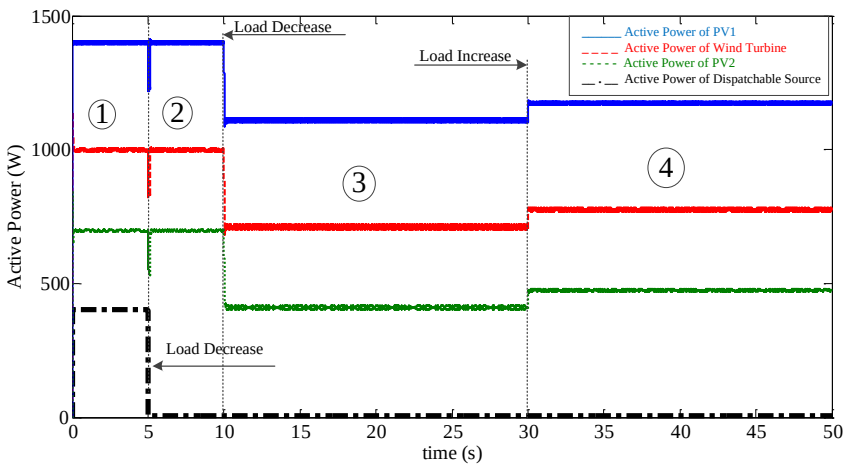



**Fig 13**. Active power variations according to load change

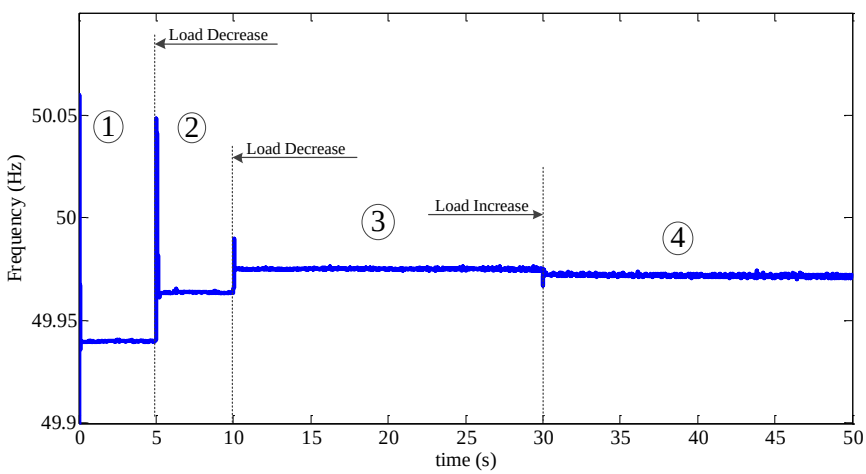



**Fig. 14.** Frequency variations according to load changes

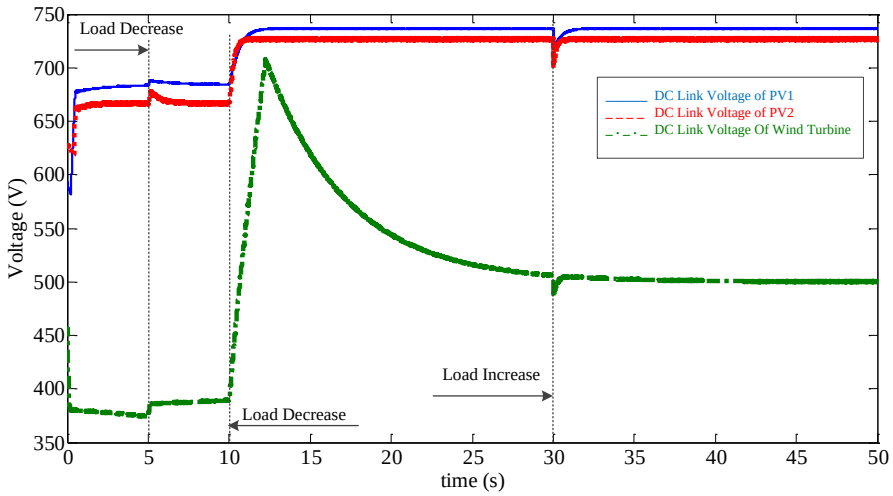



**Fig. 15.** DC-link voltage variations according to load changes

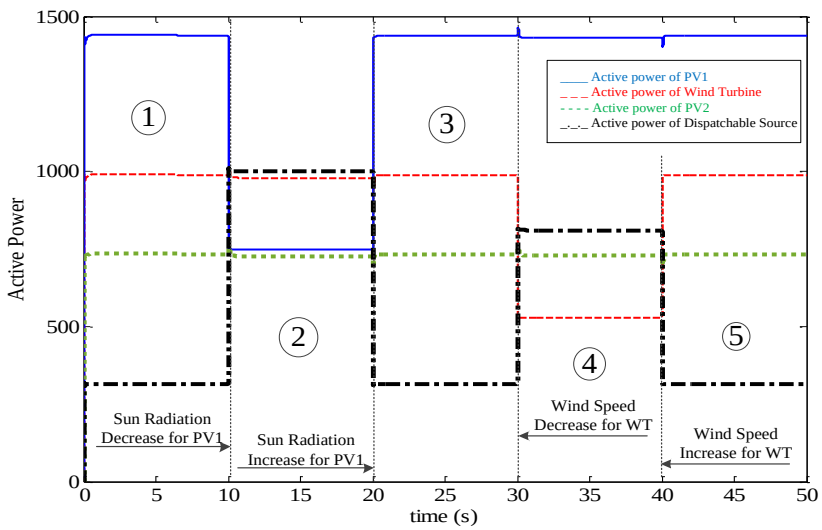



**Fig 16.** Active power variations according to weather changes

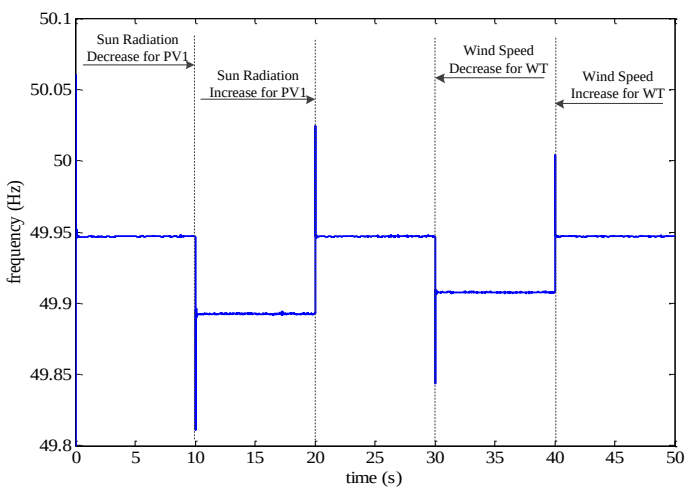



**Fig. 17.** Frequency variations according to weather changes

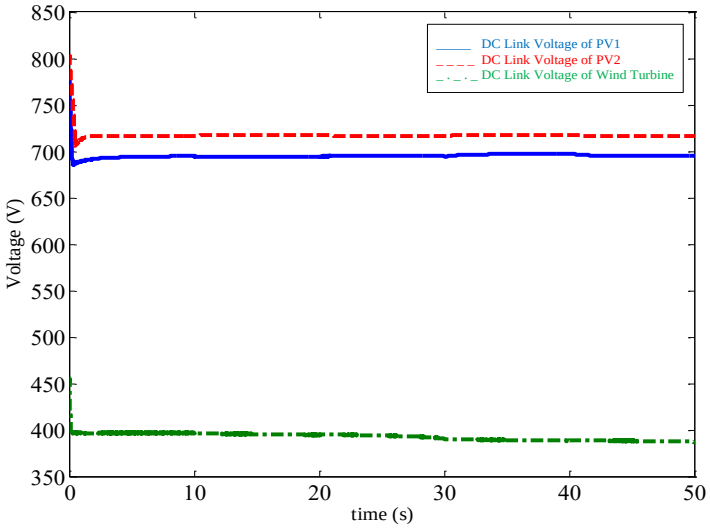



**Fig. 18.** DC-link voltage variations according to weather changes

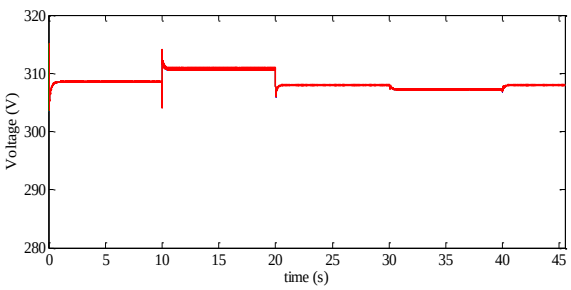



**Fig. 19.** MG voltage variations according to weather changes

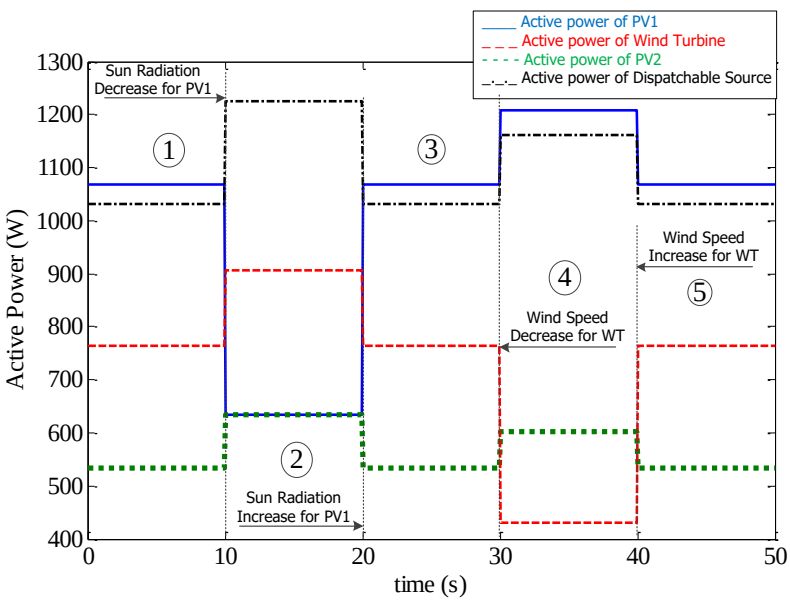



**Fig 20.** Active power variations according to weather changes with conventional droop controller

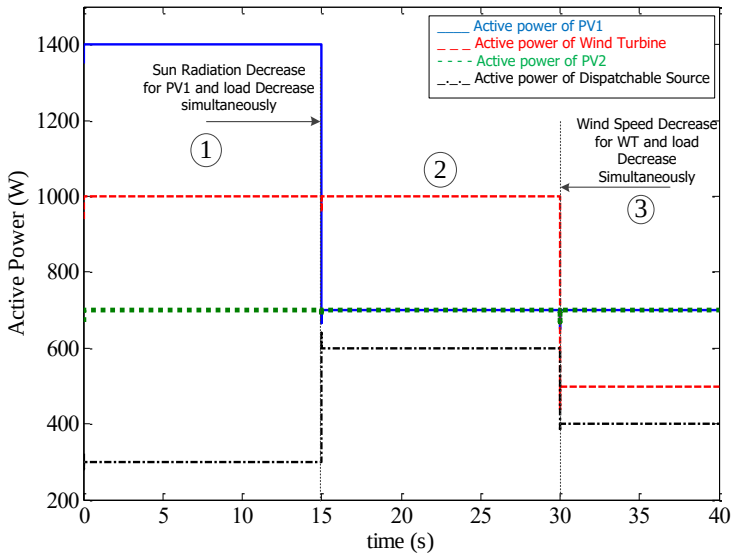



**Fig 21.** Active power variations according to weather changes and load change simultaneously with proposed droop controller

## REFERENCES


[1] C. Bustos, D. Watts and H. Ren, "MicroGrid Operation and Design Optimization With Synthetic Wins and Solar Resources," *IEEE Latin AMERICA TRANSACTIONS*, vol. 10, no. 2, pp. 1550-1562, March 2012.

[2] M. Ahmadi kamarposhti, "Optimal Control of Islanded Micro grid Using Particle Swarm Optimization Algorithm," *International Journal of Industrial Electronics, Control and Optimization (IECO)*, vol. 1, no. 1, pp. 53-60, 2018.

[3] N. Duić and M. da Graça Carvalho, "Increasing renewable energy sources in island energy supply: case study Porto Santo," *RENEWABLE AND SUSTANABLE ENERGY REVIEWS*, vol. 8, no. 4, p. 383–399, August 2004.

[4] J. M. Guerrero, J. C. Vasquez, J. Matas, L. G. d. Vicuña and M. Castilla, "Hierarchical Control of Droop-Controlled AC and DC Microgrids—A General Approach Toward Standardization," *IEEE TRANSACTIONS ON INDUSTRIAL ELECTRONICS*, vol. 58, no. 1, pp. 158-172, JANUARY 2011.

[5] J. C. Vasquez, J. M. Guerrero, M. Savaghebi, J. Eloy-Garcia and R. Teodorescu, "Modeling, Analysis, and Design of Stationary-Reference-Frame Droop-Controlled Parallel Three-Phase Voltage Source Inverters," *IEEE TRANSACTIONS ON INDUSTRIAL ELECTRONICS*, vol. 60, no. 4, pp. 1271-1280, April 2013.

[6] U. Borup, F. Blaabjerg and P. N. Enjeti, "Sharing of Nonlinear Load in Parallel-Connected Three-Phase Converters," *IEEE TRANSACTIONS ON INDUSTRY APPLICATIONS*, vol. 37, no. 6, pp. 1817-1823, November/December 2001.

[7] J. M. Guerrero, L. Hang and J. Uceda, "Control of Distributed Uninterruptible Power Supply Systems," *IEEE TRANSACTIONS ON INDUSTRIAL ELECTRONICS*, vol. 55, no. 8, pp. 2845-2859, AUGUST 2008.

[8] M. R. Patel, Wind and Solar Power System, Second ed., Tylor @ Francis, 2021.

[9] T. Ackermann, Wind Power in Power Systems, 1st ed., Stockholm: John Wiley & Sons Ltd, 2004.

[10] Y. Yang, F. Blaabjerg and H. Wang, "Constant power generation of photovoltaic systems considering the distributed grid capacity," in *IEEE APPLIED POWER ELECTRONICS CONFERENCE AND EXPOSITION*, 2014.

[11] R. Noroozian, M. Abedi, G. Gharehpetian and S. Hosseini, "Combined operation of DC isolated distribution and PV systems for supplying unbalanced AC loads," *RENEWABLE ENERGY*, vol. 34, no. 3, p. 899–908, March 2009.

[12] X. Liu, P. Wang and P. C. Loh, "Optimal coordination control for stand-alone PV system with nonlinear load," in *IPEC 2010 Conference Proceedings*, Singapore, 2010.

[13] Y. Liu, X. Zhuang, Q. Zhang, M. Arslan and H. Guo, "A novel droop control method based on virtual frequency in DC microgrid," *INTERNATIONAL JOURNAL OF ELECTRICAL POWER & ENERGY SYSTEMS*, vol. 119, 2020.

[14] R. Babazadeh-Dizaji, M. Hamzeh and A. Hekmati, "A frequency-based economical-sharing strategy for low-voltage DC microgrids," *INTERNATIONAL JOURNAL OF ELECTRICAL POWER & ENERGY SYSTEMS*, vol. 118, 2020.

[15] N. Eghtedarpour and E. Farjah, "Control strategy for distributed integration of photovoltaic and energy storage systems in DC micro-grids," *RENEWABLE ENERGY*, vol. 45, pp. 96-110, September 2012.

[16] T. Dragicevi, J. M. Guerrero, J. C. Vasquez and D. Skrlec, "Supervisory Control of an Adaptive-Droop Regulated DC Microgrid With Battery Management Capability," *IEEE TRANSACTIONS ON POWER ELECTRONICS*, vol. 29, no. 2, pp. 695 - 706, FEBRUARY 2014.

[17] H. Cai, J. Xiang and W. Wei, "Decentralized Coordination

Control of Multiple Photovoltaic Sources for DC Bus Voltage Regulating and Power Sharing," *IEEE TRANSACTION ON INDUSTRIAL ELECTRONICS*, vol. 65, no. 7, pp. 5606-5610, 2018.

[18] R. Mastromauro, M. Liserre, A. Dell'Aquila, J. Guerrero and J. Vasquez, "Droop control of a multifunctional PV inverter," in *IEEE INTERNATIONAL SYMPOSIUM ON INDUSTRIAL ELECTRONICS (ISIE)*, Cambridge, 2008.

[19] C. Trujillo Rodriguez, D. Velasco de la Fuente, G. Garcera, E. Figueres and J. Guacaneme Moreno, "Reconfigurable Control Scheme for a PV Microinverter Working in Both Grid-Connected and Island Modes," *IEEE TRANSACTION ON INDUSTRIAL ELECTRONICS*, vol. 60, no. 4, pp. 1582-1595, April 2013.

[20] X. Wang, F. Blaabjerg and Z. Chen, "Autonomous control of inverter-interfaced Distributed Generation units for harmonic current filtering and resonance damping in an islanded microgrid," *IEEE TRANSACTIONS ON INDUSTRY APPLICATIONS*, vol. 50, no. 1, pp. 452-461, JANUARY/FEBRUARY 2014.

[21] T. L. Vandoorn, B. Renders, L. Degroote, B. Meersman and L. Vandevelde, "Active Load Control in Islanded Microgrids Based on the Grid Voltage," *IEEE TRANSACTION ON SMART GRID*, vol. 2, no. 1, pp. 139-151, March 2011.

[22] Y. W. Li and C.-N. Kao, "An Accurate Power Control Strategy for Power-Electronics-Interfaced Distributed Generation Units Operating in a Low-Voltage Multibus Microgrid," *IEEE TRANSACTIONS ON POWER ELECTRONICS*, vol. 24, no. 12, pp. 2977-2988, December 2009.

[23] H. Mahmood, D. Michaelson and J. Jiang, "Strategies for Independent Deployment and Autonomous Control of PV and Battery Units in Islanded Microgrids," *IEEE JOURNAL OF EMERGING AND SELECTED TOPICS IN POWER ELECTRONICS*, vol. 3, no. 3, pp. 742-755, 2015.

[24] S. Shajari and R. Keypour, "A novel seamless droop control method for load-sharing in photovoltaic-based AC microgrids," *JOURNAL OF RENEWABLE AND SUSTAINABLE ENERGY*, vol. 11, no. 1, pp. 1-12, 2019.

[25] Y. Karimi, H. Oraee, M. S. Golsorkhi and J. M. Guerrero, "Decentralized Method for Load Sharing and Power Management in a PV/Battery Hybrid Source Islanded Microgrid," *IEEE TRANSACTIONS ON POWER ELECTRONICS*, vol. 32, no. 5, pp. 3525-3535, 2017.

[26] Y. Karimi, H. Oraee and J. M. Guerrero, "Decentralized Method for Load Sharing and Power Management in a Hybrid Single/Three-Phase-Islanded Microgrid Consisting of Hybrid Source PV/Battery Units," *IEEE TRANSACTIONS ON POWER ELECTRONICS*, vol. 32, no. 8, pp. 6135-6144, 2017.

[27] J. M. Guerrero, J. C. Vásquez, J. Matas, M. Castilla and L. G. D. Vicuña, "Control Strategy for Flexible Microgrid Based on Parallel Line-Interactive UPS Systems," *IEEE TRANSACTION ON INDUSTRIAL ELECTRONICS*, vol. 56, no. 3, pp. 726-736, March 2009.

[28] R. Sedaghati and M. R. Shakarami, "A New Sliding Mode-based Power Sharing Control Method for Multiple Energy Sources in the Microgrid under Different Conditions," *International Journal of Industrial Electronics, Control and Optimization (IECO)*, vol. 2, no. 1, pp. 25-38, 2019.

[29] G. M. Azevedo, M. C. Cavalcanti, F. A. Neves, P. Rodriguez and J. Rocabert, "Performance improvement of the droop control for single-phase inverters," in *IEEE INTERNATIONAL SYMPOSIUM ON INDUSTRIAL ELECTRONICS (ISIE)*, 2011.

[30] Q. Shafiee, J. M. Guerrero and J. C. Vasquez, "Distributed Secondary Control for Islanded MicroGrids - A Novel Approach," *IEEE TRANSACTIONS ON POWER ELECTRONIC*, vol. 29, no. 2, pp. 1018-1031, Februry 2014.

[31] A. Bidram and A. Davoudi, "Hierarchical Structure of Microgrids Control System," *IEEE TRANSACTIONS ON SMART GRID*, vol. 3, no. 4, pp. 1963-1976, DECEMBER 2012.

[32] J. Farzaneh and A. Karsaz, "Application of Improved Salp Swarm Algorithm Based on MPPT for PV Systems under Partial Shading Conditions," *International Journal of Industrial Electronics, Control and Optimization (IECO)*, vol. 3, no. 4, pp. 407-414, 2020.

[33] M. Sedaghat, A. Siadatan and B. Taheri, "Photovoltaic system with sliding mode control for work on for maximum power point," *Computational Intelligence in Electrical Engineering*, vol. 9, no. 3, pp. 76-90, 2018.

[34] C. K. Sao and W. Lehn, "Autonomous load sharing of voltage source converters," *IEEE TRANSACTION ON POWER DELIVERY*, vol. 20, p. 1009–1016, April 2005.

[35] J. Farzaneh, R. Keypour and A. Karsaz, "A novel fast maximum power point tracking for a PV system using hybrid PSO-ANFIS algorithm under partial shading conditions," *International Journal of Industrial Electronics, Control and Optimization (IECO)*, vol. 2, no. 1, pp. 47-58, winter 2019.



**Sadegh Shajari** was born in Mazandaran, Iran, in 1986. He received the B.S. and M.S degrees from the Faculty of Electrical Engineering, K. N. Toosi University of Technology both in Electrical Power System Engineering, Tehran, Iran, in 2008 and 2010 respectively. His main fields of interest were power system and Renewable Energy. He is now perusing the Ph.D. degree in the department of Electrical Engineering at Semnan University of Technology. His main research interests include hierarchical control, networked control systems, power quality and renewable energy in MicroGrids.



**Reza Keypour** received his B.Sc. degree in electrical engineering from Shahid Beheshti University in 1997 and M.Sc. and Ph.D degrees from Tarbiat modares University, Tehran, Iran in 2000 and 2006, respectively. He is currently an Associate Professor with the Faculty of Electrical and Computer Engineering, Semnan University, Semnan, Iran. His research interests include power system operation and planning, microgrids and renewable energy.

**IECO**

**This page intentionally left blank.**